

Domain wall propagation and nucleation in a metastable two-level system

Hans C. Fogedby

Institute of Physics and Astronomy, University of Aarhus,
DK-8000, Aarhus C, Denmark

and

NORDITA, Blegdamsvej 17,
DK-2100, Copenhagen, DenmarkJohn Hertz^yNORDITA, Blegdamsvej 17,
DK-2100, Copenhagen, DenmarkAxel Svane^zInstitute of Physics and Astronomy, University of Aarhus,
DK-8000, Aarhus C, Denmark

(Dated: March 22, 2024)

We present a dynamical description and analysis of non-equilibrium transitions in the noisy one-dimensional Ginzburg-Landau equation for an extensive system based on a weak noise canonical phase space formulation of the Freidlin-Wentzel or Martin-Siggia-Rose methods. We derive propagating nonlinear domain wall or soliton solutions of the resulting canonical field equations with superimposed diffusive modes. The transition pathways are characterized by the nucleations and subsequent propagation of domain walls. We discuss the general switching scenario in terms of a dilute gas of propagating domain walls and evaluate the Arrhenius factor in terms of the associated action. We find excellent agreement with recent numerical optimization studies.

PACS numbers: 05.40.-a, 05.45.Yv, 05.20.-y

I. INTRODUCTION

Phenomena far from equilibrium are ubiquitous, including turbulence in fluids, interface and growth problems, chemical and biological systems, and problems in material science and nanophysics. In this context the dynamics of complex systems driven by weak noise, corresponding to rare events, is of particular interest. The issue of different time scales does in fact characterize many interesting processes in nature. For instance, in the case of chemical reactions the reaction time is often orders of magnitude larger than the molecular vibration periods [1]. The time scale separation problem is also encountered in the case of conformational changes of biomolecules, nucleation events during phase transitions, switching of the magnetization in magnetic materials [2, 3], and even in the case of comets exhibiting rapid transitions between heliocentric orbits around Jupiter [4].

The weak noise limit, characterizing the time scale separation, is associated with the strong coupling regime, and the problem of determining kinetic pathways and transition probabilities between metastable states in systems with many degrees of freedom presents one of the most important and challenging tasks in many areas of physics [5]. The long time scales are associated with the separation in energy scales of the thermal energy and the energy barriers between metastable states; the transition takes place by sudden jumps between metastable states followed by long waiting times in the vicinity of the states. The fundamental issue is thus the determination of transition pathways and the associated transition rates.

In the weak noise limit the standard Monte Carlo method or direct simulation of the Langevin equation becomes impractical owing to the large separation of time scales and alternative methods have been developed. The most notable analytical approach is the formulation due to Freidlin and Wentzel which yields the transition probabilities in terms of an action functional [6]. This approach is the analogue of the variational principle proposed by Machlup and Onsager [7, 8], see also work by Graham et al. [9, 10]. The Freidlin-Wentzel approach is equivalent to the Martin-Siggia-Rose method [11] in the weak noise limit of the path integral formulation [12, 13, 14, 15, 16]. In order

^Electronic address: fogedby@phys.au.dk

^yElectronic address: hertz@nordita.dk

^zElectronic address: svane@phys.au.dk

to overcome the time scale gap various numerical methods have also been proposed. We mention here the transition path sampling method [17] and optimization techniques [18, 19].

A particularly interesting non-equilibrium problem of relevance in the nanophysics of switches is the influence of thermal noise on two-level systems with spatial degrees of freedom, see Refs. [2, 3, 20]. In a recent paper by E, Ren, and Vanden-Eijnden [21], see also Ref. [19], this problem has been addressed using the Ginzburg-Landau equation driven by thermal noise. Applying the field theoretic version of the Onsager-Machlup functional [7, 8] in the Freidlin-Wentzell formulation [6], these authors implement a powerful numerical optimization techniques for the determination of the space-time configuration minimizing the Freidlin-Wentzell action and in this way determine the kinetic pathways and their associated action, yielding the switching probabilities in the long time-low temperature limit. The picture that emerges from this numerical study is that of noise-induced nucleation and subsequent propagation of domain walls across the sample, giving rise to the switch between metastable states.

In recent work we have addressed a related problem in non-equilibrium physics, namely the Kardar-Parisi-Zhang equation or equivalent noisy Burgers equation describing, for example, a growing interface in a random environment. Using a canonical phase space method derived from the weak noise limit of the Martin-Siggia-Rose functional or directly from the Fokker-Planck equation, we have, in the one dimensional case, analyzed the coupled field equations minimizing the action both analytically [22, 23, 24, 25, 26, 27] and numerically [28]. The picture that emerges is that the transition probabilities in the weak noise limit are associated with soliton propagation and nucleation resulting from soliton collisions.

In the present paper we apply the canonical phase space approach to the noisy Ginzburg-Landau equation discussed by E, Ren, and Vanden-Eijnden [21] and attempt to account for some of their numerical findings. We thus give analytical arguments for the propagation of noise-induced solitons and the nucleation events originating from soliton annihilation and creation. The paper is organized in the following way. In Sec. II we introduce the noisy Ginzburg-Landau equation. In Sec. III we review the canonical phase space approach. In Sec. IV we discuss dispersive mode and domain wall solutions of the field equations replacing the noisy Ginzburg-Landau equation. In Sec. V we analyze the domain wall dynamics. In Sec. VI we present a stochastic interpretation of our results. In Sec. VII we discuss equilibrium properties and kinetic transitions. In Sec. VIII we present an interpretation of the numerical results obtained by the optimization studies of E et. al [21]. Sec. IX is devoted to a summary and a conclusion. A brief version of the present work has appeared in Ref. [29].

II. THE NOISY GINZBURG - LANDAU MODEL

The noisy Ginzburg-Landau equation driven by white noise has the form

$$\frac{\partial u}{\partial t} = -\frac{F}{u} + \xi; \quad (2.1)$$

where the locally correlated Gaussian white noise is specified by the moment

$$\langle \xi(x;t) \xi(0;0) \rangle = \delta(x) \delta(t); \quad (2.2)$$

with noise strength parameter ϵ . The free energy F providing the deterministic drive is given by

$$F = \frac{1}{2} \int dx \left[\left(\frac{\partial u}{\partial x} \right)^2 + V(u) \right]; \quad (2.3)$$

In the switching problem considered by E et al. [21] the double well potential $V(u)$ has the form

$$V(u) = k_0^2 (1 - u(x)^2)^2; \quad (2.4)$$

with strength parameter k_0 . The potential vanishes at the two minima $u = \pm 1$ and assumes the maximum value $V(0) = k_0^2$ at $u = 0$. The time scale is set by the kinetic transport coefficient ϵ and the dimensionless scalar field u determines the spatial and temporal state of the switch. The "Mexican hat" double well potential is depicted in Fig. 1

The Ginzburg-Landau equation in its deterministic form has been used both in the context of phase ordering kinetics [30] and in its complex form in the study of pattern formation [31]. In the noisy case for a finite system the equation has been studied in [32]; see also an analysis of the related ϕ^4 theory in [33]. In the present problem the noisy equation provides a generalization of the classical Kramers problem [5] to spatially extended systems.

By inspection of Eqs. (2.1), (2.2), and (2.3) we note that k_0 has the dimension of an inverse length, ϵ the dimension of length squared over time, and ϵk_0 the dimension of velocity. For large k_0 , which is the case considered here, and

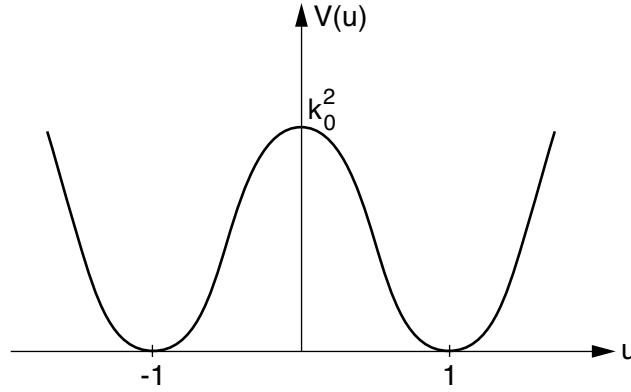


FIG. 1: We depict the double-well potential defining the unperturbed states of the switch. The potential has minima at $u = \pm 1$ and a maximum at $u = 0$.

for $\beta = 0$ the potential term dominates the dissipative term and the field u locks on to the values ± 1 in bulk; imposed boundary values being accommodated over a saturation or healing length of order k_0^{-1} . In the presence of noise the minima become unstable to thermal fluctuations and the noise can drive the system over the potential barrier.

The Ginzburg-Landau equation (2.1) admits a fluctuation-dissipation theorem yielding the stationary distribution

$$P_{\text{stat}} \propto \exp \left[-\frac{2}{T} F \right] \quad (2.5)$$

In a thermal environment at temperature T we have $\beta = 2/T$ (in units such that $k_B = 1$) and $P_{\text{stat}} \propto \exp[-F/T]$, i.e., the Boltzmann distribution. The equilibrium states follow from the condition

$$\frac{\delta F}{\delta u} = -r^2 u - 2k_0^2 u(1 - u^2) = 0; \quad (2.6)$$

yielding two degenerate uniform ground states $u = \pm 1$ with free energy $F = 0$, as well as two nonuniform domain wall solutions

$$u_{\text{dw}}(x) = \tanh k_0(x - x_0); \quad (2.7)$$

centered at x_0 and of width k_0^{-1} . For large $|x|$ the domain wall solutions overlap with the uniform ground state solutions $u = \pm 1$. The associated domain wall free energy is

$$F_{\text{dw}} = 4k_0 = 3; \quad (2.8)$$

The minima, maxima, and saddle point structure of the complex energy landscape of F as a functional of $fu(x)$ are inferred from the spectrum of the differential operator

$$\frac{\delta^2 F}{\delta u^2} = -r^2 - 2k_0^2(1 - 3u^2); \quad (2.9)$$

For the ground states $u = \pm 1$ the spectrum of $\delta^2 F / \delta u^2$ is given by the plane wave mode $\exp(ikx)$ with positive eigenvalues $k^2 + 4k_0^2$. For a single domain wall configuration or n connected domain walls the spectrum is composed of zero-eigenvalue translation modes (Goldstone modes) and superimposed phase shifted plane wave modes

$\exp[ikx] \exp(i\theta)$ with positive eigenvalues $k^2 + 4k_0^2$, see e.g. Ref. [34]. We thus infer that the free energy landscape possesses two global minima at $u = \pm 1$ and a series of local saddle points of free energy $4nk_0 = 3$, corresponding to n connected domain walls at positions $x_i; i = 1; 2; \dots; n$. In Fig. 2 we have depicted a static 3-domain wall configuration connecting the ground states $u = -1$ and $u = +1$ with free energy $4k_0$. The static single domain wall or multi-domain wall configurations correspond to points in the free energy landscape $F = F(fu(x))$ and cannot effectuate a switch between the ground state configurations $u = \pm 1$. However, in the presence of noise the Kramers escape mechanism sets in and the system can perform a kinetic transition. The transition probability is typically characterized by an Arrhenius factor $P \propto \exp[-F/T]$ where F is the free energy associated with the potential barriers encountered in the dynamic transition, see e.g. [5]. In order to address this issue for the noisy Ginzburg-Landau equation we apply the canonical phase space approach.

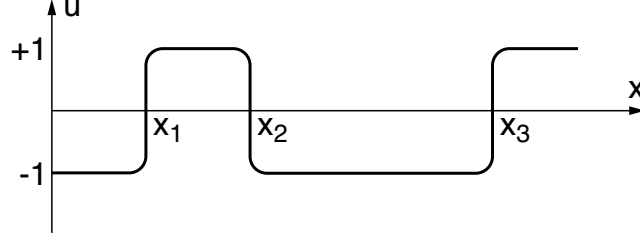


FIG. 2: We depict a static 3-domain wall configuration connecting the ground states $u = -1$ and $u = +1$. The domain walls are located at x_1 , x_2 , and x_3 . The configuration corresponds to a saddle point in the free energy landscape and has free energy $4k_0$.

III. THE CANONICAL PHASE SPACE APPROACH

The canonical phase space approach is discussed in detail in [28, 35]. Briefly, the Fokker-Planck equation for the probability distribution $P(u(x); t)$ has the general form

$$\frac{\partial P}{\partial t} = H P; \quad (3.1)$$

with formal solution $P = \exp[H t]$. The Fokker-Planck equation (3.1) is driven by the Hamiltonian or Liouvilian $H(u; \dot{u})$ (a differential-functional operator in $u(x)$ space). The method is based on a weak noise WKB-like approximation

$$P \sim \exp \left[-\frac{S}{\epsilon} \right]; \quad (3.2)$$

applied to Eq. (3.1). To leading order in the noise strength the action S satisfies the Hamilton-Jacobi equation

$$\frac{\partial S}{\partial t} + H(p; u) = 0; \quad (3.3)$$

with canonical momentum $p = \delta S / \delta \dot{u}$, defining the Hamiltonian H as a functional of u and p and implying a principle of least action. The variational principle $\delta S = 0$, moreover, implies the Hamiltonian field equations of motion

$$\frac{\partial u}{\partial t} = \frac{\delta H}{\delta p}; \quad (3.4)$$

$$\frac{\partial p}{\partial t} = -\frac{\delta H}{\delta u}; \quad (3.5)$$

and the action

$$S = \int_{t_1}^{t_2} dx dt p \frac{\partial u}{\partial t} - \int_{t_1}^{t_2} dt H; \quad (3.6)$$

Applying this scheme to the Ginzburg-Landau equation (2.1) we obtain

$$\frac{\partial u}{\partial t} = -\frac{F}{u} + p; \quad (3.7)$$

$$\frac{\partial p}{\partial t} = -\frac{\delta F}{\delta u^2} p; \quad (3.8)$$

driven by the Hamiltonian (the generator of time translations)

$$H = \int dx H = \frac{1}{2} \int dx p^2 - \int dx \frac{F}{u}; \quad (3.9)$$

with $F = u$ and ${}^2F = u^2$ given by Eqs. (2.6) and (2.9). As a result the action S associated with an orbit from u_1 to u_2 traversed in time T is given by

$$S(u_1; u_2; T) = \int_{u_1; 0}^{u_2; T} dx dt \, p \frac{\partial u}{\partial t} - H; \quad (3.10)$$

where H is the Hamiltonian density. In our further analysis we shall also make use of the total momentum (the generator of space translations)

$$P = \int dx \, u \frac{\partial p}{\partial x}; \quad (3.11)$$

The prescription for determining the relevant Arrhenius factor associated with a transition and the kinetic pathway is thus straightforward. Fixing boundary values in space and time the first step is to solve the coupled field equations (3.7) and (3.8) for an orbit (a minimizer in the terminology of Ref. [21]) from u_1 to u_2 traversed in time T , next we evaluate the action S along an orbit according to Eq. (3.10), and finally deduce the transition probability from Eq. (3.2).

The correspondence with the equivalent Freidlin-Wentzel action S_{FW} is obtained by inserting the equation of motion (3.7) and the Hamiltonian (3.9) in the action (3.10), yielding $S = (1/2) \int dx dt p^2$ or $S_{FW} = (1/2) \int dx dt (\partial u / \partial t + F = u)^2$. The Freidlin-Wentzel method is a Lagrangian configuration space method with Lagrangian density $L = (1/2) (\partial u / \partial t + F = u)^2$, whereas the present approach is a phase space formulation with action (3.10). We also note that the equations of motion (3.7) and (3.8) are identical to the saddle point equations in the Martin-Siggia-Rose functional formulation [11, 14].

IV. DIFFUSIVE MODE AND DOMAIN WALL SOLUTIONS

More explicitly, inserting $F = u$ and ${}^2F = u^2$ from Eqs. (2.6) and (2.9) the equations of motion (3.7) and (3.8) assume the form

$$\frac{\partial u}{\partial t} = \frac{\partial^2 u}{\partial x^2} + 2k_0^2 u(1 - u^2) + p; \quad (4.1)$$

$$\frac{\partial p}{\partial t} = \frac{\partial^2 p}{\partial x^2} - 2k_0^2 p(1 - 3u^2); \quad (4.2)$$

and the Hamiltonian is

$$H = \frac{1}{2} \int dx \, p^2 + 2 \int dx \, \frac{\partial^2 u}{\partial x^2} + 4k_0^2 u(1 - u^2); \quad (4.3)$$

The equations of motion (4.1) and (4.2) determine orbits in a multi-dimensional phase space $(u(x); p(x))$ lying on the energy manifolds determined by Eq. (4.3); for open or periodic boundary conditions the orbits are moreover confined by the conservation of the total momentum given by Eq. (3.11). From an analytical point of view the field equations (4.1) and (4.2) are in general intractable. Even numerically, the negative diffusion term in Eq. (4.2) renders the coupled equations highly unstable as was noted in the numerical analysis of the Burgers equation [28].

A. Linear diffusive modes

It is instructive first to consider the easily discussed linear case of simple diffusion for small k_0 . Thus ignoring the non-linear potential terms in Eqs. (4.1) and (4.2) we obtain the linear equations

$$\frac{\partial u}{\partial t} = \frac{\partial^2 u}{\partial x^2} + p; \quad (4.4)$$

$$\frac{\partial p}{\partial t} = \frac{\partial^2 p}{\partial x^2}; \quad (4.5)$$

generated by the Hamiltonian

$$H = \frac{1}{2} \int dx \, p^2 + 2 \int dx \, \frac{\partial^2 u}{\partial x^2}; \quad (4.6)$$

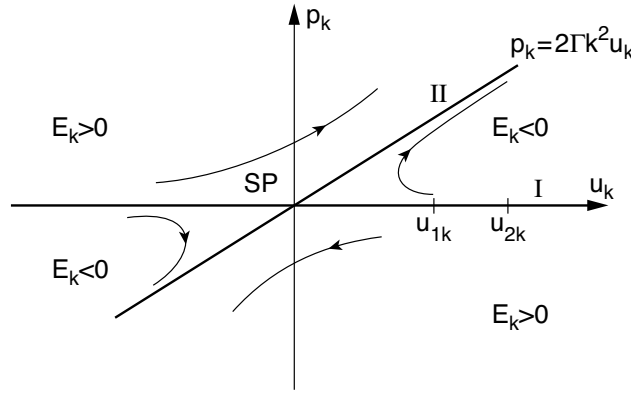


FIG. 3: We show the orbits in the $(u_k; p_k)$ phase space. The finite time orbit from u_{1k} to u_{2k} lies on the energy manifold $E_k = p_k [p_k - 2k^2 u_k]$. In the long time limit $T \rightarrow \infty$ the orbits migrate to the transient manifold $p_k = 0$ (I) and the stationary manifold $p_k = 2k^2 u_k$ (II) passing through the saddle point $(u_k; p_k) = (0; 0)$ (SP) implying ergodicity and a stationary state.

In Fourier space, setting $u_k = \int_{-\infty}^{\infty} dx \exp(-ikx) u$ and $p_k = \int_{-\infty}^{\infty} dx \exp(-ikx) p$, $u_k = u_k$ and $p_k = p_k$, the equations of motion decompose and we arrive at the orbit solution, see Ref. [35],

$$u_k(t) = \frac{u_{2k} \sinh k^2 t + u_{1k} \sinh k^2 (T-t)}{\sinh k^2 T}; \quad (4.7)$$

from u_{1k} at time $t=0$ to u_{2k} at time $t=T$; $u_{1,2} = \int_{-\infty}^{\infty} (dk/2) \exp(ikx) u_{1,2,k}$. The noise field p_k is slaved to the motion of u_k and given by

$$p_k(t) = k^2 e^{k^2 t} \frac{u_{2k} e^{-k^2 T}}{\sinh k^2 T}; \quad (4.8)$$

Likewise, the Hamiltonian H decomposes into independent k -mode contributions

$$H = \int \frac{dk}{2} p_k [p_k - 2k^2 u_k]; \quad (4.9)$$

Inserting the solutions (4.7) and (4.8) we obtain specially for the energy of the k -th mode

$$E_k = \frac{(k^2)^2}{2} \frac{u_{2k}^2 + u_{1k}^2 - 2u_{1k}u_{2k} \cosh k^2 T}{\sinh^2 k^2 T}; \quad (4.10)$$

The orbits lie on the energy manifolds given by $E_k = p_k [p_k - 2k^2 u_k]$. In the long time limit $T \rightarrow \infty$ the orbits migrate to the zero-energy manifolds consisting of the transient submanifold $p_k = 0$ and the stationary submanifold $p_k = 2k^2 u_k$, and pass asymptotically through the hyperbolic fixed point at $(u_k; p_k) = (0; 0)$, determining the stationary state. In Fig. 3 we have shown the orbits for a particular k -mode in a plot of p_k versus u_k .

Finally, the conserved momentum and the action S follow from Eqs. (3.11) and (3.10)

$$= \int \frac{dk}{2} (-ik) p_k u_k; \quad (4.11)$$

and

$$S = \int \frac{dk}{2} k^2 \frac{u_{2k} u_{1k} e^{-k^2 T}}{1 - e^{-2k^2 T}}; \quad (4.12)$$

yielding the transition probability from u_{1k} to u_{2k} in time T ,

$$P(u_{1k}; u_{2k}; T) / \exp \left[- \int \frac{dk}{2} k^2 \frac{u_{2k} u_{1k} e^{-k^2 T}}{1 - e^{-2k^2 T}} \right]; \quad (4.13)$$

In the long time limit $T \rightarrow \infty$ we reach the stationary distribution

$$P_{st}(f u_k g) / \exp \left(- \frac{1}{2} \int \frac{dk}{2\pi} k^2 |u_k|^2 \right) : \quad (4.14)$$

This result is consistent with the noise-driven diffusion equation written in the form $\partial u / \partial t = \nabla^2 (F = u + \frac{1}{2} \nabla^2 u^2)$, with free energy $F = (1/2) \int dx (\partial u / \partial x)^2$. Invoking the fluctuation-dissipation theorem we then obtain an equilibrium distribution given by the Boltzmann factor $\exp(-F/T)$, $T = 2$, consistent with Eq. (4.14).

In summary, in the linear purely diffusive case the configurations $u(x;t)$ decompose into independent k -modes. In the dynamical phase space approach the noise ξ_k driving the individual k -modes is replaced by the noise field p_k which couples parametrically to the time evolution of the u_k mode. In a transient time regime u_k is damped according to the diffusion equation and the orbit in phase space lies close to the transient or noiseless submanifold $p_k = 0$ and approaches the saddle point $(u_k; p_k) = (0; 0)$. At longer times the growing noise field p_k drives u_k away from the saddle point and the orbit approaches the stationary or noisy submanifold $p_k = 2 k^2 u_k$, i.e., the distribution associated with the noise-driven diffusion equation approaches a stationary distribution. In the limit $T \rightarrow \infty$ the orbit passes asymptotically through the saddle point and the orbit from u_{1k} to u_{2k} lies on the zero-energy manifold determining the stationary state.

B. Domain wall modes

In the nonlinear case the phase space representation of the noise-driven Ginzburg-Landau equation is given by the coupled field equations (4.1) and (4.2) determining the orbits. As in the linear case we can identify the zero-energy submanifolds determining the stationary state. This is related to the existence of a fluctuation-dissipation theorem for the noisy Ginzburg-Landau equation (2.1) expressed by the existence of a free energy. From the Hamiltonian (3.9) we infer tentatively the zero-energy submanifolds $p = 0$ and $p = 2 F = u$. The transient noiseless submanifold $p = 0$ is consistent with the equations of motion and the configurations decay according to the damped deterministic Ginzburg-Landau equation

$$\frac{\partial u}{\partial t} = - \frac{F}{u} : \quad (4.15)$$

Note that in contrast to the linear case where the u configurations decompose in k -modes which decay according to $u_k \sim \exp(-k^2 t)$, an initial configuration u_1 in the nonlinear case will in general decay forming a pattern of interacting and annihilating domain wall configurations with superimposed diffusive modes.

The stationary submanifold $p = 2 F = u$ inserted in Eqs. (3.7) and (3.8) yields the equations

$$\frac{\partial u}{\partial t} = - \frac{F}{u}; \quad (4.16)$$

$$\frac{\partial p}{\partial t} = 2 \frac{F}{u} - \frac{F^2}{u^2}; \quad (4.17)$$

which are consistent since $\partial u / \partial t = -(1/2)p$. It is interesting to notice that the motion of u on the stationary noisy submanifold $p = 2 (F = u)$ is a time-reversed version of the motion on the transient submanifold $p = 0$. Finally, on the zero-energy manifold the action in Eq. (3.6) takes the form $S = \int dx dt p \partial u / \partial t = 2 \int dx dt (\partial u / \partial t) (F = u) = 2 F$, yielding the stationary distribution in Eq. (2.5) for the noisy Ginzburg-Landau equation.

In the absence of a fluctuation-dissipation theorem as is for example the case for the kinetic KPZ equation or, equivalently, noisy Burgers equation, we can in general not explicitly identify the stationary zero-energy submanifold and thus simply determine the stationary state; an exception is the KPZ equation in 1D where for special reasons a fluctuation-dissipation theorem is available, see Refs. [23, 24, 35].

In order to address non-equilibrium properties such as a specific transition probability from an initial state u_1 to a final state u_2 in passage time T we must address the nonlinear equations of motion (4.1) and (4.2). The field equations are not integrable and do not yield to a general analytical solution. However, we can advance our understanding by first searching for static solutions on the transient manifold $p = 0$, i.e., the solution of the equation $F = u = 0$ yielding according to Eq. (2.6) the domain wall solutions in Eq. (2.7). The domain wall excitations are of the instanton type and can be located at arbitrary positions, see Ref. [36]. Since the overlap between two well-separated domain walls is exponentially small we can construct approximate multi-domain wall solutions of the form

$$u_{dw} = \sum_{i=1}^N \tanh k_0 (x - x_i) + u_0; \quad (4.18)$$

$$p_{dw} = 0; \quad (4.19)$$

Here the parity index $\epsilon_i = \pm 1$ for right hand and left hand domain walls, respectively, and x_i indicates the center of the domain wall. The offset $u_0 = 0$ for multi-domain wall configurations overlapping for large $|x|$ with two different ground state configurations and $u_0 = \pm 1$ for configurations overlapping with identical ground states $u = \pm 1$, respectively. Assuming that the inter-domain wall distance $|x_i - x_{i+1}|$ is large compared with the domain wall width $l=k_0$, i.e., the case of a dilute domain wall gas, the expression (4.18) constitutes an approximate solution to Eq. (2.6). Since the domain wall solutions are associated with the transient submanifold $p = 0$ it also follows from Eqs. (4.3), (3.11) and (3.10) that they carry vanishing energy, momentum, and action within the canonical phase space approach.

V. DOMAIN WALL DYNAMICS

In order to impart dynamical attributes to the domain walls and thus provide solutions to the coupled field equations (4.1) and (4.2) we perform a linear stability analysis about the static domain wall solutions.

A. Dynamics of a single domain wall

Setting $u = u_{dw} + \tilde{u}$ and $p = p_{dw} + \tilde{p}$, $p_{dw} = 0$ in Eqs. (4.1) and (4.2) we obtain to linear order the coupled equations

$$\frac{\partial \tilde{u}}{\partial t} = \frac{\partial^2 \tilde{u}}{\partial x^2} + 2k_0^2(1 - 3u_{dw}^2)\tilde{u} + \tilde{p}; \quad (5.1)$$

$$\frac{\partial \tilde{p}}{\partial t} = \frac{\partial^2 \tilde{p}}{\partial x^2} - 2k_0^2(1 - 3u_{dw}^2)\tilde{p}; \quad (5.2)$$

Noting that in a Schrodinger equation analogue the domain wall profile u_{dw} gives rise to a Bargmann type potential Eqs. (5.1) and (5.2) are readily analyzed, see e.g. Ref. [34]. Expanding \tilde{u} and \tilde{p} on the eigenfunctions ψ_n of the Schrodinger operator

$$D = -\partial^2 + 2k_0^2 - 2 \frac{3}{\cosh^2 k_0 x}; \quad (5.3)$$

according to

$$\tilde{u} = \sum_n \tilde{u}_n \psi_n; \quad (5.4)$$

$$\tilde{p} = \sum_n \tilde{p}_n \psi_n; \quad (5.5)$$

the time-dependent expansion coefficients \tilde{u}_n and \tilde{p}_n are determined by the coupled equations of motion

$$\frac{d\tilde{u}_n}{dt} = \epsilon_n \tilde{u}_n + \tilde{p}_n; \quad (5.6)$$

$$\frac{d\tilde{p}_n}{dt} = -\epsilon_n \tilde{p}_n; \quad (5.7)$$

where ϵ_n is the eigenvalue in the eigenvalue equation $D \psi_n = \epsilon_n \psi_n$. Equations (5.6) and (5.7) have the same structure as the Fourier transformed versions of Eqs. (4.4) and (4.5) in the case of the linear dispersive modes, and the solutions are given by Eqs. (4.7) and (4.8) with k^2 replaced by ϵ_n . The canonical phase space structure with k^2 replaced by ϵ_n is depicted in Fig. 3.

The spectrum of D in Eq. (5.3) is composed of two bound states ψ_0 and ψ_1 with eigenvalues $\epsilon_0 = 0$ and $\epsilon_1 = 3k_0^2$, respectively, and a band of phase-shifted plane wave solutions ψ_k with eigenvalues $\epsilon_k = k^2 + 4k_0^2$

$$\psi_0 = \frac{3k_0}{4} \frac{1}{\cosh^2 k_0 x}; \quad \epsilon_0 = 0; \quad (5.8)$$

$$\psi_1 = \frac{3k_0}{2} \frac{\sinh k_0 x}{\cosh^2 k_0 x}; \quad \epsilon_1 = 3k_0^2; \quad (5.9)$$

$$\psi_k = \frac{1}{2} e^{ikx} s_k(x); \quad \epsilon_k = k^2 + 4k_0^2; \quad (5.10)$$

$$s_k(x) = \frac{k^2 + k_0^2 - 3k_0^2 \tanh^2 k_0 x + 3ikk_0 \tanh k_0 x}{(k - ik_0)(k - 2ik_0)}; \quad (5.11)$$

The complex space-dependent smatrix $s_k(x)$ gives rise to a space and phase modulation of the plane wave mode. For $x \rightarrow 1$ we have $s_k(x) \rightarrow 1$, whereas for $x \rightarrow -1$ we obtain $s_k(x) \rightarrow \exp(i\phi_0(k)) \exp(i\phi_1(k))$ where the phase shifts $\phi_0 = 2 \tan^{-1}(k_0/k)$ and $\phi_1 = 2 \tan^{-1}(2k_0/k)$ are associated with the depletion of the band due to the formation of the bound states ϕ_0 and ϕ_1 , respectively. In terms of the expansion coefficients u_n and p_n the Hamiltonian H , momentum P , and action S in Eqs. (4.3), (3.11), and (3.10) are given by

$$H = \frac{1}{2} \sum_n p_n (p_n - 2 u_n u_n); \quad (5.12)$$

$$P = \sum_n p_n \int dx u_{dw} r_n \quad (5.13)$$

$$S = \frac{1}{2} \sum_n \int dx \dot{p}_n p_n; \quad (5.14)$$

expressing the dynamics of the various modes.

1. Domain wall motion

The mode ϕ_0 with eigenvalue $\omega_0 = 0$ plays a special role since it is associated with the uniform translation of the domain wall. For $\omega_0 = 0$ the equation of motions (5.6) and (5.7) take the form $du_0/dt = p_0$ and $dp_0/dt = 0$ with solutions $u_0 = p_0 t$, $p_0 = \text{cst.}$ For the field u associated with the mode ϕ_0 we have $u = u_{dw} + u_0$. Inserting ϕ_0 and $u_0 = p_0 t$ we obtain

$$u = u_{dw} + p_0 t - \frac{3k_0}{4} \frac{1}{k_0^2} r u_{dw} / u_{dw}(x - vt); \quad (5.15)$$

describing a domain wall propagating with velocity

$$v = \frac{3}{4k_0} \frac{1}{k_0^2}; \quad \omega_0 = 0. \quad (5.16)$$

The mode ϕ_0 is the well-known translation or Goldstone mode restoring the broken translation symmetry associated with the localized domain wall mode. In the present canonical formulation the translation mode also implies the propagation of the domain wall.

It is also instructive to consider the noise field p which in the dynamical description corresponds to the noise η . In the case of a single domain wall we obtain from Eq. (5.5) a static configuration. It is, however, clear that the noise field must move together with the domain wall configurations and we conclude that terms beyond linear order give rise to a renormalization of the noise field implying a finite propagation velocity, i.e.,

$$p / p_0 = \frac{1}{\cosh^2 k_0(x - vt)}; \quad (5.17)$$

The noise field is thus localized at the position of the domain wall corresponding to a noise impulse associated with the formation of the domain wall. In Fig. 4 we have depicted a single moving right hand domain wall (index $i = 1$) with associated noise field. The dynamics of a single domain wall follows from Eqs. (5.12), (5.13), and (5.14); we have

$$E_0 = \frac{1}{2} p_0^2; \quad (5.18)$$

$$\omega_0 = \frac{4k_0}{3} \frac{1}{k_0^2}; \quad (5.19)$$

$$S_0 = \frac{1}{2} T p_0^2; \quad (5.20)$$

In terms of the propagation velocity v we have $\omega_0 = (4/3)k_0 v$ and we can associate an effective mass $(4/3)k_0$ with the domain wall motion,

$$m = \frac{4}{3} k_0; \quad (5.21)$$

note that the mass vanishes in the limit of a broad domain wall.

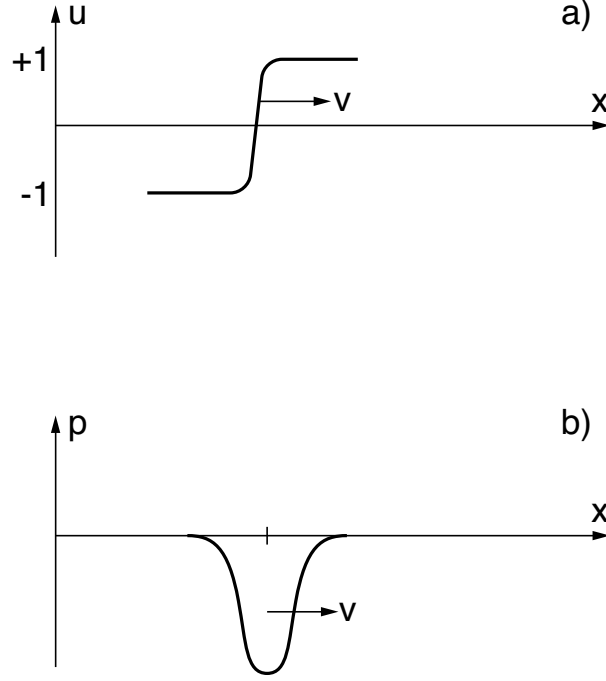


FIG. 4: In a) we show a right hand domain wall in u moving with velocity v . In b) we depict the associated impulsive noise field p

2. Deformation and extended modes

The bound state ψ_1 given by (5.9) is odd and accounts for the symmetrical deformation of the moving domain wall. The time-dependence of u is given by Eqs. (4.7) and (4.8) with k^2 replaced by $k_1^2 = 3k_0^2$. The band of plane wave solutions in Eq. (5.10) corresponds to corrections to the leading and trailing edges of the domain wall. The modes have dispersive character with growing and damped time behavior and are given by Eqs. (4.7) and (4.8) with k^2 replaced by $(k^2 + 4k_0^2)$; note that in the limit $k_0 \rightarrow 0$ we recover the linear case. The extended modes are phase-shifted $2 \tan^{-1}(k_0/k) + 2 \tan^{-1}(2k_0/k)$ which by Levinson's theorem corresponds to the two bound states, the translation mode and deformation mode, being depleted from the band.

B. Dynamics of multi-domain wall configurations

In the multi-domain wall case the analysis proceeds in a similar manner. Expanding about the static multi-domain wall configuration in Eqs. (4.18) and (4.19), $u = u_{dw} + \tilde{u}$ and $p = p_{dw} + \tilde{p}$, $p_{dw} = 0$, we obtain for a dilute domain wall gas the coupled linear equations

$$\frac{\partial \tilde{u}}{\partial t} = \frac{\partial^2 \tilde{u}}{\partial x^2} + 2k_0^2 \tilde{u} + 3 \sum_{i=1}^N \frac{1}{\cosh^2 k_0(x - x_i)} \tilde{u} + \tilde{p}; \quad (5.22)$$

$$\frac{\partial \tilde{p}}{\partial t} = \frac{\partial^2 \tilde{p}}{\partial x^2} - 2k_0^2 \tilde{p} + 3 \sum_{i=1}^N \frac{1}{\cosh^2 k_0(x - x_i)} \tilde{p}; \quad (5.23)$$

which are analyzed in terms of the spectrum of the Schrodinger operator

$$D = -\nabla^2 + 2k_0^2 - 3 \sum_{i=1}^N \frac{1}{\cosh^2 k_0(x - x_i)}; \quad (5.24)$$

with identical well-separated potential wells at x_i . Expanding u and p on the eigenfunctions ϕ_n of D , $D\phi_n = -\omega_n^2 \phi_n$, we recover the equations of motion (5.6) and (5.7).

The eigenstates ϕ_n are readily expressed as linear superpositions of the eigenstates for the individual potential wells and we obtain the translation modes ϕ_0 with eigenvalue $\omega_0^2 = 0$, the deformation modes ϕ_1 with eigenvalue $\omega_1^2 = 3k_0^2$, and the extended plane wave modes ϕ_k with eigenvalues $\omega_k^2 = k^2 + 4k_0^2$,

$$\phi_0 = \sum_{i=1}^N A_0^i \phi_0^i; \quad \phi_0^i = \frac{1}{\cosh^2 k_0 (x - x_i)}; \quad (5.25)$$

$$\phi_1 = \sum_{i=1}^N A_1^i \phi_1^i; \quad \phi_1^i = \frac{\sinh k_0 (x - x_i)}{\cosh^2 k_0 (x - x_i)}; \quad (5.26)$$

$$\phi_k = e^{ikx} \sum_{i=1}^N A_k^i \phi_k^i; \quad A_k^i(x) = \frac{k^2 + k_0^2}{(k - ik_0)(k + 2ik_0)} \left(\frac{3k_0^2 \tanh^2 k_0 x + 3ik_0 \tanh k_0 x}{k - ik_0} \right); \quad (5.27)$$

In terms of the individual eigenfunctions the expansions of u and p take the form

$$u = \sum_{ni} u_{ni} \phi_n^i; \quad u_{ni} = u_n A_i; \quad (5.28)$$

$$p = \sum_{ni} p_{ni} \phi_n^i; \quad p_{ni} = p_n A_i; \quad (5.29)$$

and we obtain the equations of motion

$$\frac{du_{ni}}{dt} = -\omega_n u_{ni} + p_{ni}; \quad (5.30)$$

$$\frac{dp_{ni}}{dt} = -\omega_n p_{ni}; \quad (5.31)$$

with solutions given by Eqs. (4.7) and (4.8). Moreover, the dynamics of a multi-domain wall configuration is given by

$$H = \frac{1}{2} \sum_{ni} p_{ni}^2 - \sum_{ni} \omega_n^2 u_{ni}^2; \quad (5.32)$$

$$= \sum_{ni} p_{ni} \frac{dx_{dw}^i}{dt}; \quad (5.33)$$

$$S = \frac{1}{2} \sum_{ni} \int dt p_{ni} \dot{p}_{ni}; \quad (5.34)$$

For the translation mode in particular we have $\dot{u}_{0i} = \dot{p}_{0i} = 0$, yielding $u_{0i} = p_{0i}t$ and we obtain

$$u = u_{dw} + p_{0i}t \frac{3k_0}{4} \frac{1}{k_0^2} r_{dw} / u_{dw}(x - vt); \quad (5.35)$$

with propagation velocity

$$v_i = p_{0i} \frac{3}{4k_0} \frac{1}{k_0^2}; \quad (5.36)$$

Likewise, the dynamics of the domain wall at x_i is given by

$$E_{0i} = \frac{1}{2} p_{0i}^2; \quad (5.37)$$

$$p_{0i} = p_{0i} \frac{4k_0}{3} \frac{1}{k_0^2}; \quad (5.38)$$

$$S_0 = \frac{1}{2} T p_{0i}^2; \quad (5.39)$$

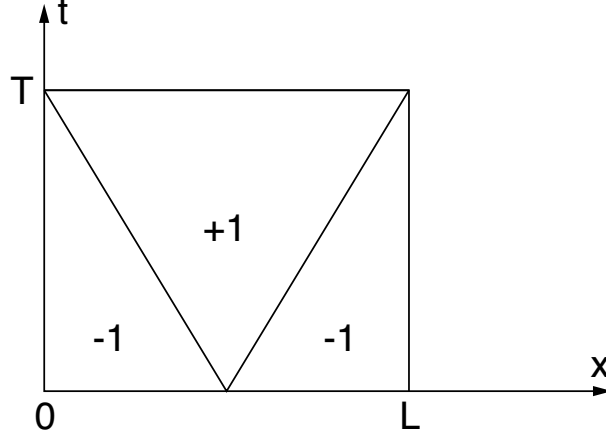


FIG. 5: We show the transition from the ground state $u = -1$ to the ground state $u = +1$ in a system of size L in time T due to the nucleation of a domain wall pair at the center of the system.

Summarizing, the linear analysis of the static domain wall configuration leads to a picture of a dilute gas of propagating domain walls. Superposed on the domain walls are localized deformation modes and extended modes of dispersive character. The time evolution of the domain wall-linear mode gas is moreover subject to three constraints: 1) the topological signature of the domain walls implies that a right hand domain wall is matched to a consecutive left hand domain wall, 2) translational invariance implies that the total momentum given by Eq. (5.33) is conserved, and 3) finally, time translation invariance entails that the total energy E given by Eq. (5.32) is a constant of motion.

C. Domain wall nucleation and annihilation

The above analysis of the dynamics of the domain wall-dispersive mode system is restricted to the dilute gas regime. However, the topological constraints together with the conservation laws allow a heuristic analysis of domain wall collisions. When a right hand domain wall collides with a left hand domain wall the topological constraint implies that they must annihilate to the uniform ground states $u = +1$ or $u = -1$. Moreover, since Eq. (3.11) implies that the momentum $= 0$ for $u = -1$, the domain wall pair prior to collision must move with equal and opposite momenta, i.e., equal and opposite velocities. Since the phase space formulation is time reversal invariant we also infer that pairs of oppositely moving domain walls of opposite parity can nucleate out of the uniform ground states $u = -1$. In the ground state Eq. (4.3) implies that the energy is given by $E = (1/2) \int dx p^2$. Consequently, in order to generate domain wall pairs out of the ground state we must assign a finite noise field p . In Fig. 5 we have in a plot of t versus x depicted the transition from the state $u = -1$ to the state $u = +1$ due to the formation of a domain wall pair. The system is of size L and the transition takes place in time T . In Fig. 6 we have shown the corresponding propagation of the domain wall pair receding from the nucleation zone with opposite velocities together with the associated noise field. According to Eqs. (5.16) and (5.17) the noise field profiles moving with the domain walls are positive and have the form $1 = \cosh^2 k_0(x - vt)$

VI. STOCHASTIC INTERPRETATION

The domain wall gas picture introduced above allows a systematic dynamical approach to the determination of kinetic pathways and to the evaluation of the Arrhenius factors associated with the transitions. The approach moreover permits a straightforward stochastic interpretation making contact with the customary discussion of the noisy Ginzburg-Landau equation.

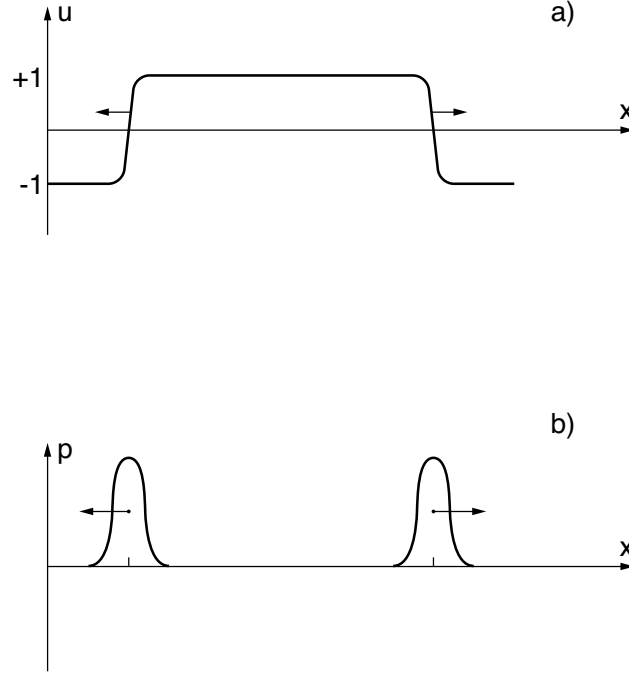


FIG. 6: In a) we show the domain wall pair propagating away from the nucleation zone. In b) we show the associated comoving noise field profiles.

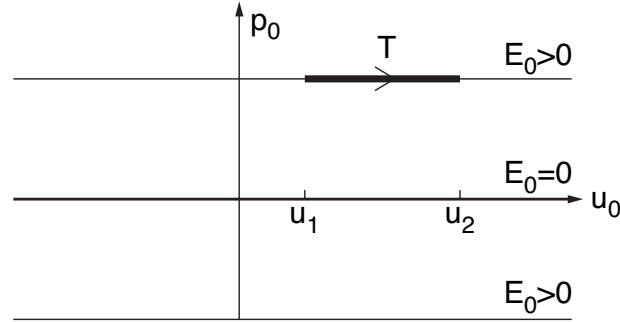


FIG. 7: We show the orbits in the $(u_0; p_0)$ phase space in the case of domain wall motion. The finite-time orbits lie on the finite energy manifolds $E_0 = (1/2)p_0^2$. In the long time limit $T \rightarrow \infty$ the orbit from u_1 to u_2 migrates to the zero-energy manifold $E_0 = 0$.

A. Domain wall random walk

In the case of a single domain wall the dynamics follows from Eqs. (5.6) and (5.7) for $\phi_0 = 0$, i.e., the equations of motion $du_0/dt = p_0$ and $dp_0/dt = 0$ with solutions $u_0 = p_0 t$, $p_0 = \text{constant}$. The energy E_0 , momentum p_0 and action S_0 are given by (5.18), (5.19), and (5.20), respectively, and the orbits lie on the energy manifolds $E_0 = (1/2)p_0^2$. In Fig. 7 we have depicted the phase space for the motion of a single domain wall. The plot depicts orbits from u_1 to u_2 in time T on the manifold $E_0 = (1/2)p_0^2$. In the long time limit the orbits migrate to the zero-energy manifold $E_0 = 0$. The phase space plot is a degenerate limit of the phase space plot in Fig. 3 for $k_0 \rightarrow 0$. We note the absence of a stationary zero-energy manifold and saddle point yielding a stationary state. Since the momentum p_0 according to Eq. (5.19) is proportional to the canonical momentum p_0 it follows directly from the canonical structure that the conjugate variable to u_0 is the center of mass position x_0 of the domain wall. From the Poisson bracket $\{u_0, p_0\} = 1$

and $\dot{x}_0; \dot{y}_0 = 1$ together with $\dot{y}_0 = (4k_0=3)^{1/2} p_0$, we infer $u_0 = m^{1/2} x_0, m = 4k_0=3$, and the ensuing equation of motion

$$m \frac{dx_0}{dt} = 0; \quad (6.1)$$

with solution

$$x_0 = \frac{0}{m}t + \text{constant}; \quad (6.2)$$

Likewise, the energy and action are given by $E_0 = \frac{0}{2} = 2m$ and

$$S_0 = T \frac{0}{2m}; \quad (6.3)$$

The stochastic interpretation of the phase space dynamics readily follows. Considering an orbit from x_1 to x_2 traversed in time T , corresponding to the propagation of a domain wall with center of mass position x_1 at time $t=0$ to the center of mass position x_2 at time $t=T$, and inserting the solution (6.2) in Eq. (5.20) we obtain

$$S_0 = \frac{1}{2} m \frac{(x_2 - x_1)^2}{T}; \quad (6.4)$$

yielding the transition probability from x_1 to x_2 in the time interval T

$$P(x_1; x_2; T) / \exp \left[-\frac{m}{2} \frac{(x_2 - x_1)^2}{T} \right]; \quad (6.5)$$

This is the Gaussian distribution for random walk with root mean square deviation $x_{rms} = (2T/m)^{1/2}$, $m = 4k_0=3$. We note that the distribution in Eq. (6.5) is obtained in the limit $\hbar \rightarrow 0$ from the overdamped oscillator distribution in Eq. (4.13). We conclude that the uniform or ballistic motion of a domain wall within the dynamical description corresponds precisely to ordinary random walk of the domain wall within the associated stochastic description.

The random walk behavior of a domain wall also follows easily from the Ginzburg Landau equation (2.1). Inserting the fluctuating domain wall ansatz $u(x;t) = \tanh k_0(x - x(t))$, where $x(t)$ is the time-dependent center of mass x and noting that $F = u = 0$ for a domain wall we obtain, integrating over space, setting $\dot{x}(t) = dx/dt$ (x;t),

$$\frac{dx(t)}{dt} = \dot{x}(t); \quad (6.6)$$

which is the Langevin equation for random walk.

It is also straightforward to include the contribution to the stochastic behavior from the deformation and dispersive modes associated with the domain wall. From Eq. (4.12) applied to the local deformation mode (def) u_1 and the dispersive modes (di) u_k we obtain for the total action for a dressed domain wall

$$S = S_0 + S_{\text{def}} + S_{\text{di}}; \quad (6.7)$$

where S_0 is given by Eq. (6.4) and S_{dm} and S_b by

$$S_{\text{def}} = 3 k_0^2 \frac{(u_{21} - u_{11} e^{3 k_0^2 T})^2}{1 - e^{6 k_0^2 T}}; \quad (6.8)$$

$$S_{\text{di}} = \sum_k \frac{dk}{2} (k^2 + 4k_0^2) \frac{j_{12k} u_{1k} e^{(k^2 + 4k_0^2)T}}{1 - e^{2(k^2 + 4k_0^2)T}}; \quad (6.9)$$

For the transition probability from an initial dressed domain wall configuration $u_1(x) = f(x_1; u_{11}; u_{1k})$ to a final dressed domain wall configuration $u_2(x) = f(x_2; u_{21}; u_{2k})$ during the time interval T we finally obtain

$$P(u_1; u_2; T) = P_0 P_{\text{def}} P_{\text{di}}; \quad (6.10)$$

where P_0 is given by Eq. (6.5) and $P_{\text{def}} / \exp[-S_{\text{def}}]$ and $P_{\text{di}} / \exp[-S_{\text{di}}]$. In the long time limit $t \rightarrow \infty$ the domain wall performs a random walk, whereas the deformation mode and dispersive modes attain a stationary state, i.e.,

$$P(x; T; u_1; f u_k) / \exp \left[-\frac{m x^2}{2 T} \right] \exp \left[-\frac{3 k_0^2 u_1^2}{2} \right] \exp \left[-\sum_k \frac{dk}{2} (k^2 + 4k_0^2) j_{1k}^2 \right]; \quad (6.11)$$

B . D o m a i n w a l l g a s

In the case of a dilute domain wall gas with associated linear modes the discussion above applies in a generalized form. From Eqs. (5.30) and (5.31) for $\eta_0 = 0$ we obtain the equations of motion $du_{0i}/dt = p_{0i}$ and $dp_{0i}/dt = 0$ with solutions $u_{0i} = p_{0i}t + \text{cst}$, $p_{0i} = \text{cst}$. The energy, momentum, and action are given by Eqs. (5.37), (5.38), and (5.39), respectively, and each domain wall lies on the corresponding energy manifold $E_{0i} = (1/2)p_{0i}^2$. For each domain wall the phase space plot in Fig. 4 thus applies. Since the action in (5.34) is additive with a contribution from each domain wall the transition probabilities factorize and we obtain for the random walk part from (6.5)

$$P(\mathbf{f}x_{i1}g; \mathbf{f}x_{i2}g; T) / \prod_i \exp \left(-\frac{m(\mathbf{x}_{i2} - \mathbf{x}_{i1})^2}{2T} \right) : \quad (6.12)$$

Likewise, the contributions from the deformation and dispersive modes follow from Eqs. (6.8) and (6.9).

V I I . K I N E T I C T R A N S I T I O N S

In the previous sections we have established the dynamical framework in the case of the noise-driven Ginzburg-Landau equation and established the connection to the customary stochastic interpretation. In summary, the domain wall gas picture provides a description of a switching scenario in terms of moving right hand and left hand domain walls with associated linear modes. The dynamical approach moreover implies that the kinetic pathway from an initial configuration to a final configuration is associated with a specific orbit in canonical phase space. The action associated with the orbit yields the Arrhenius factor associated with the transition. The domain wall gas picture shows that a class of orbits, i.e., a class of solutions of the field equations can be parametrized in terms of a dilute gas of propagating domain walls with superimposed local deformation and extended phase-shifted dispersive modes. This picture is derived from a linear analysis and only holds a priori in a dilute gas limit and at short times. As discussed below the domain wall dynamics at later times can be extracted heuristically from a combination of selection rules and conservation laws.

A . E q u i l i b r i u m

Before we discuss kinetic transitions it is instructive first briefly to discuss the equilibrium properties. In equilibrium the free energy landscape is determined by the structure of $F(u)$ in Eq. (2.3). The complex landscape is characterized by the presence of two global minima corresponding to the uniform ground states $u = +1$ and $u = -1$ and an infinity of saddle points corresponding to static nonuniform multi-domain wall configurations. The flat parts of the saddle points correspond to the translation modes associated with the domain walls. The free energy $F = 0$ for the ground states. For an n -domain wall configuration $F = nm$, where the mass $m = 4k_0/3$. In Fig. 8 we have sketched the free energy landscape associated with a single static domain wall connecting $u = -1$ and $u = +1$. In the case of zero noise for $\eta = 0$ the system starting from an arbitrary initial configuration $u_1(x)$ approaches the state with lowest free energy compatible with the imposed boundary conditions. The relaxational dynamics is governed by Eq. (4.15) and corresponds in the dynamical approach to an orbit connected to the $p = 0$ zero-energy submanifold. For open or periodic boundary conditions the configurations with lowest free energy are the two degenerate uniform ground states $u = \pm 1$. Imposing vanishing boundary conditions $u = 0$ at $x = 0$ and $x = L$ for a system of size L the field u grows to the uniform values $u = \pm 1$ or $u = +1$ over a healing length of order $l = k_0$. Imposing periodic boundary conditions we infer that the healing profile corresponds to a half domain wall and that the free energy of the configuration equals $2m = (1/2)m = m$. Finally, for skew boundary conditions with $u = -1$ for $x = 0$ and $u = +1$ for $x = L$ the state with lowest free energy corresponds to a single domain wall with free energy m . The different scenarios are depicted in Fig. 9. In the presence of noise for $\eta \neq 0$ the ground states become metastable and the system populates the excited states with $F \neq 0$. The partition function provides a global characterization of the equilibrium excursions in the free energy landscape and is according to Eq. (2.5) given by

$$Z = \sum_{\text{fug}} \exp \left(-\frac{2}{\eta} F(u) \right) ; \quad (7.1)$$

where the configuration fug has the free energy $F(u)$, yielding the Boltzmann factor in Eq. (7.1). The evaluation of Z and associated correlations, e.g., $\langle u_i(x;t) u_j(x;t) \rangle$ in the dilute non-overlapping domain wall gas limit follows closely the well-known soliton and instanton methods developed in the seventies and used in Ref. [34] for the classical easy-plane

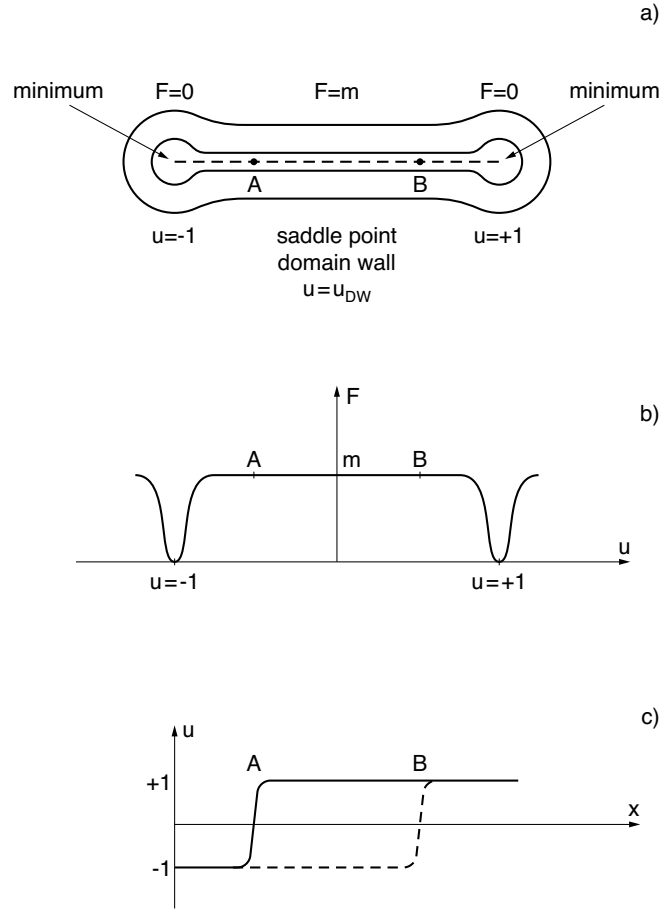


FIG. 8: In a) we have in a contour plot sketched the free energy landscape in the case of a single static domain wall overlapping for large $j_{\text{D}}/j_{\text{W}}$ with the ground states $u = -1$ and $u = +1$. The points A and B indicate two distinct positions of the domain wall, corresponding to the translation mode. In b) we have sketched the free energy as function of u . The u axis labels collectively the $u(x)$ configurations in the free energy landscape. The points A and B refer to the domain wall positions. Since the free energy of the domain wall is independent of the center of mass position the landscape exhibits a constant F ridge. In c) we have depicted the corresponding domain wall configurations at center of mass positions A and B.

ferromagnet. Expanding the free energy defined by Eqs. (2.3) and (2.4) about an n -domain wall configuration we have, setting $u = u_{dw} + u$, $F = F(u_{dw}) + (l=2) u D u$. Using $F(u_{dw}) = nm$, inserting D from Eq. (5.24), and expanding u on the eigenfunctions χ_n , we obtain

$$F = nm + \frac{1}{2} \sum_n \chi_n^2 : (7.2)$$

Introducing a domain wall chemical potential μ_{dw} in order to control the domain wall densities we arrive at the grand partition function

$$Z = 2 \exp \left(\frac{2}{n} (\mu_{dw} - m) \right) \frac{1}{n!} \sum_{i=1}^Z \int du_{0i} \int du_{1i} \int du_{ki} \exp \left(- \sum_{i=1}^Z \left(u_{0i}^2 + u_{1i}^2 + \sum_k \mu_{ki}^2 \right) \right) : (7.3)$$

The overall factor 2 arises from the double degeneracy of the ground state and the domain walls connecting the ground states. The $\mu_0 = 0$ eigenvalue yields the translation mode and it follows that $du_{0i} = m^{1/2} dx_i$, where x_i is the position of the i -th domain wall. The factor $1/n!$ takes into account the ordering of the domain walls when integrating x_i over a system of size L . Performing the Gaussian integrals over the deformation and dispersive modes we have in more

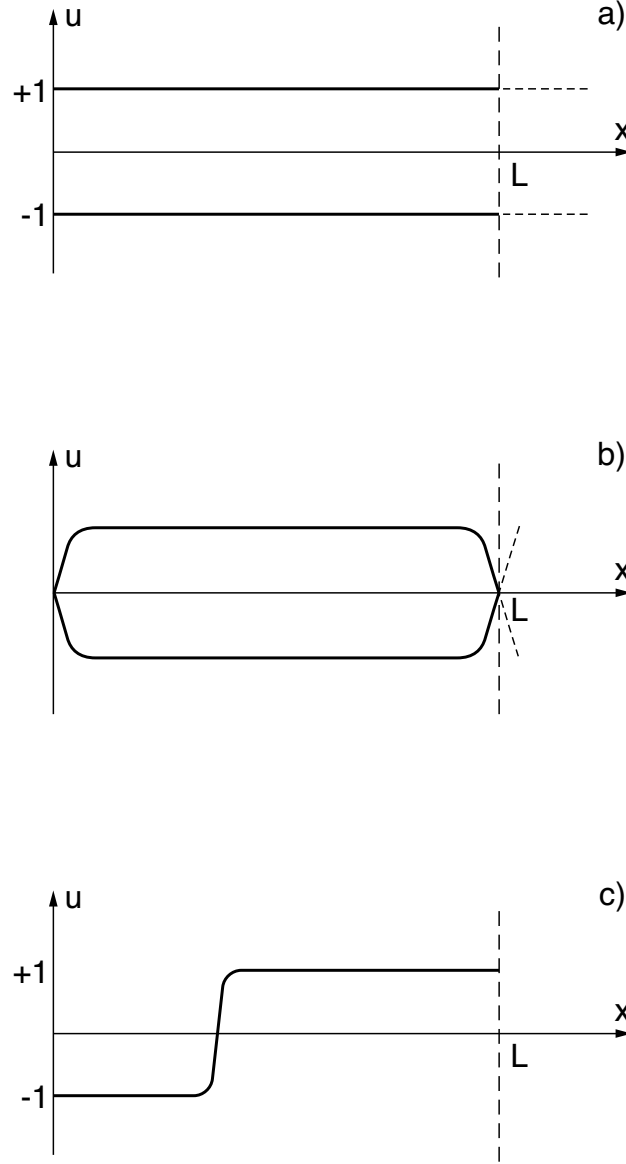


FIG. 9: In a) we have shown the ground state configurations with $F = 0$ in the case of open or periodic boundary conditions. In b) the lowest configuration with fixed boundary conditions have $F = m$. In c) we show the lowest spatially degenerate domain wall configuration with $F = m$ in the case of skew boundary conditions.

reduced form

$$Z = 2 \sum_{n=0}^{\infty} \frac{1}{n!} \exp \left(\frac{2}{n} \left(\frac{m}{L} \right)^n \right) \frac{1}{n!} \exp \left(\frac{1}{2} \sum_k \log \frac{1}{k} \right) : \quad (7.4)$$

We have introduced the large wavenumber UV cutoff in order to regularize Z at small distances. Note that in the treatment in Ref. [34] the lattice distance of the magnetic chain provided a natural small scale cutoff. Replacing the summation over k by an integral according to the prescription $\sum_k \rightarrow \int \frac{dk}{2\pi}$, where the density of states $\rho(k) = \frac{1}{2\pi} \left(1 + \frac{1}{k^2} \right)$, and summing over domain walls the partition function factorizes into a disusive part and a domain wall part, incorporating also the contribution from the localized deformation modes,

$$Z = Z_{\text{di}} Z_{\text{dw}}; \quad (7.5)$$

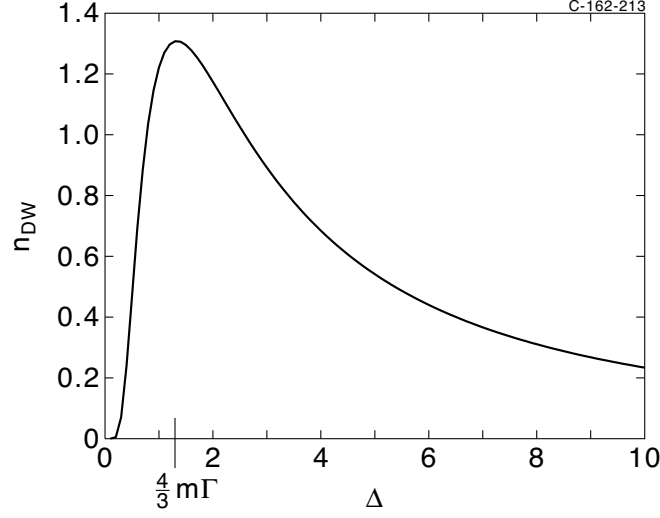


FIG. 10: We show the domain wall density n_{dw} in units of $\beta=2$ as function of the noise strength Δ in units of m . The density vanishes in the limits $\Delta \rightarrow 0$ and $\Delta \rightarrow 1$ and exhibits a maximum at $4m = 3$.

$$Z_{di} = \exp \frac{L}{2} \log \frac{1}{\pi} ; \quad (7.6)$$

$$Z_{dw} = 2 \exp -8Lk_0^{3=2} \frac{1=2}{\exp \frac{2}{m} (n_{dw} - m)} : \quad (7.7)$$

In a thermal environment $\beta = 2/T$ and the partition function gives direct access to e.g., the specific heat. We shall not pursue this calculation here except noting that the gap in the domain wall excitation spectrum gives rise to a Schottky anomaly in the specific heat, see e.g., Ref. [34]. Noting that the number of domain walls accessed by the stationary fluctuations is undetermined it is, however, instructive to evaluate the domain wall density n_{dw} . From the structure of Z we infer $n_{dw} = (\beta=2) (d \log Z / d \Delta)_{\Delta=0}$ and inserting Eqs. (7.5), (7.6), and (7.7) we obtain, setting $k_0 = 3m = 4, x \rightarrow f$

$$n_{dw} = 8 \frac{1=2}{\frac{3}{4}m} \frac{3=2}{\exp \frac{2}{m}} : \quad (7.8)$$

The domain wall density vanishes in the limits $\Delta \rightarrow 0$ and $\Delta \rightarrow 1$ and exhibits a maximum for $\Delta = 4/3$. We have depicted n_{dw} as a function of Δ in Fig. 10.

B. Transitions in the Kramers case

Before turning to the noise-induced kinetic transitions in the Ginzburg-Landau equation it is instructive to review the classical Kramers theory [5, 37] for a single degree of freedom, which can be analyzed completely, and its formulation within the canonical phase space approach.

1. Kramers theory

We consider the overdamped case characterized by the Langevin equation for one degree of freedom u

$$\frac{du}{dt} = -\frac{dF}{du} + \xi ; \quad (7.9)$$

$$h(u(t)) - h(u(0)) = -\int_0^t \frac{dF}{du} du + \int_0^t \xi(u) du ; \quad (7.10)$$

with kinetic coefficient and noise strength γ ; in thermal equilibrium $\gamma = 2/T$, where T is the temperature. For the free energy F we assume a double well profile with maximum $F(0)$ at $u = 0$ and minima at $u = \pm 1$ with $F(\pm 1) = 0$. The free energy is depicted in Fig. 11 a). The Fokker-Planck equation associated with Eqs. (7.9) and (7.10) has the form

$$\frac{\partial P}{\partial t} = \frac{1}{2} \frac{\partial^2 P}{\partial u^2} + \frac{\partial}{\partial u} \left(\frac{dF}{du} P \right) \quad (7.11)$$

We note the stationary state for $\partial P / \partial t = 0$

$$P_{st} \propto \exp \left(-\frac{2}{\gamma} F \right); \quad (7.12)$$

in accordance with Eq. (2.5), showing how the free energy profile is globally sampled in the stationary state.

In order to evaluate the transition rate from, say, the state $u = -1$ to the state $u = +1$ across the free energy barrier $F(0)$ we follow Kramers and set up a constant probability current J across the barrier generated by a source to the left of the barrier in region A and absorbed by a sink to the right of the barrier in region B. From the conservation law $\partial P / \partial t + \partial J / \partial u = 0$ and Eq. (7.11) we derive the current

$$J = -\frac{1}{2} \frac{\partial P}{\partial u} - \frac{dF}{du} P \quad (7.13)$$

Assuming a sink at $u_+ > 0$ we obtain the steady state solution

$$P(u) = \frac{2J}{\gamma} \exp \left(-\frac{2}{\gamma} F(u) \right) \int_u^{u_+} du^0 \exp \left(-\frac{2}{\gamma} F(u^0) \right) \quad (7.14)$$

Setting up a population $n = \int_{-1}^{R_0} du P(u)$ to the left of the barrier the rate is given by $k = J/n$ and we have

$$k^{-1} = \frac{2}{\gamma} \int_{-1}^{R_0} du \exp \left(-\frac{2}{\gamma} F(u) \right) \int_u^{u_+} du^0 \exp \left(-\frac{2}{\gamma} F(u^0) \right) \quad (7.15)$$

Finally, a simple steepest descent calculation for $\gamma \rightarrow 0$ yields Kramers celebrated result for the rate in the overdamped Smoluchowski limit, $F''(0) = d^2F/du^2$,

$$k = \frac{\gamma}{2} (F''(0))^{1/2} \exp \left(-\frac{2}{\gamma} F(0) \right) \quad (7.16)$$

The rate is determined by the Arrhenius factor $\exp(-2/\gamma F(0))$ depending on the height of the barrier and the prefactor $(\gamma/2) (F''(0))^{1/2}$. Here the double derivative $F''(0)$ can be associated with the oscillation frequencies in the potential well at $u = \pm 1$ and about the maximum at $u = 0$

2. Dynamical interpretation of Kramers theory

Here we discuss the Kramers escape problem from a potential well within the canonical phase space method. According to the general formulation in Sec. III the Hamiltonian associated with the Langevin equation (7.9) has the form

$$H = \frac{1}{2} p^2 - \frac{\gamma}{2} \frac{dF}{du} u \quad (7.17)$$

yielding the equations of motion

$$\frac{du}{dt} = \frac{dF}{du} + p; \quad (7.18)$$

$$\frac{dp}{dt} = -\frac{d^2F}{du^2} p; \quad (7.19)$$

and the associated action

$$S(u; T) = \int_{-1}^{u_+} dt p \frac{du}{dt} - H \quad (7.20)$$

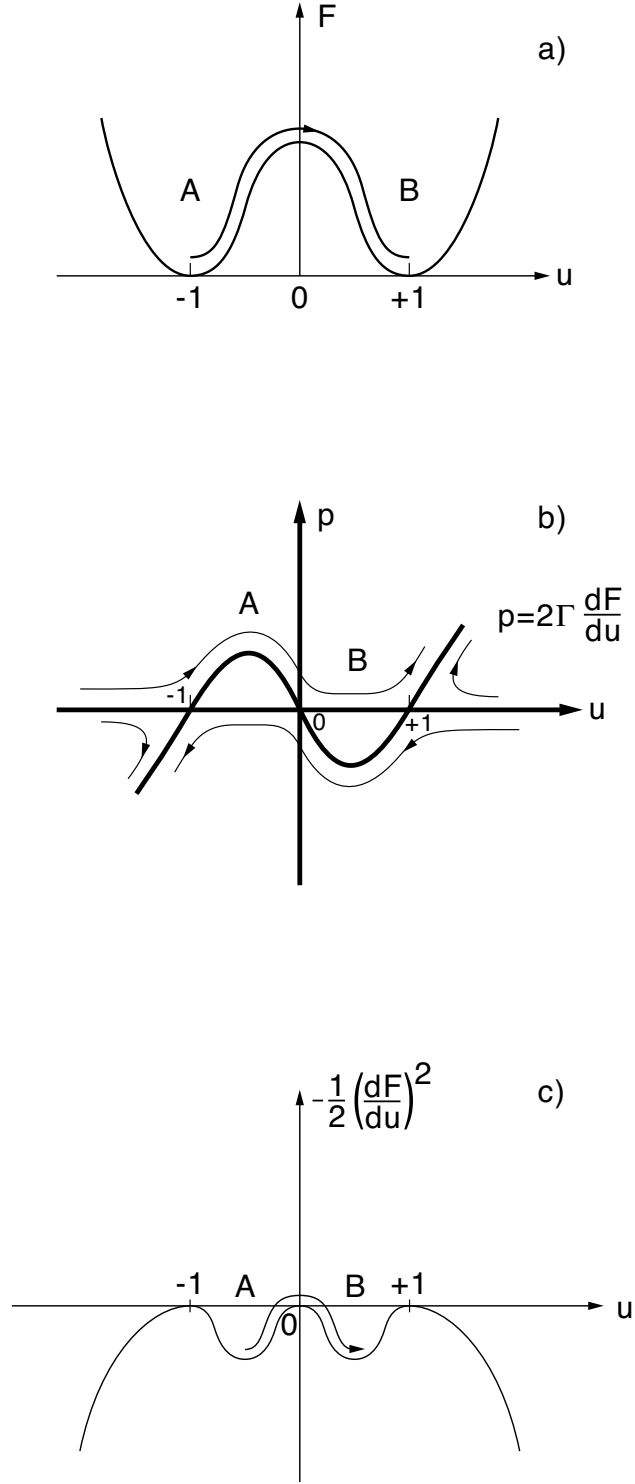


FIG. 11: In a) we show the double well structure of the free energy F . In b) we show orbits in the canonical phase space. The zero-energy manifolds are $p = 0$ and $p = 2\Gamma \frac{dF}{du}$, intersecting at the saddle points $(u; p) = (-1; 0)$, $(0; 0)$, and $(1; 0)$. In c) we show the inverted double well potential entering in the Newton equation description of the transition.

For the normalized transition probability we have

$$P(u;T) = \frac{\int_{u_i}^{u_f} \exp\left(-\frac{S(u;T)}{\hbar}\right) du}{\int_{u_i}^{u_f} \exp\left(-\frac{S(u;T)}{\hbar}\right) du} \quad (7.21)$$

In Fig. 11 b) we have depicted the phase space for the Kramers escape case. The zero-energy manifolds are given by $p = 0$ and $p = 2 \, dF/du$. On the phase space plot we have shown an orbit from region A to region B, i.e., across the free energy barrier. Comparing Fig. 11 a) with Fig. 11 b) we note that the "uphill" part of the orbit in region A is controlled by the $p = 2 \, dF/du$ manifold whereas the "downhill" part in region B is controlled by the $p = 0$ manifold. In the long time limit the orbit approaches the zero-energy manifolds $p = 0$ and $p = 2 \, dF/du$ passing close to the saddle points at $u = -1$, $u = 0$, and $u = 1$. A simple calculation along the "bulge" setting $H = 0$ and inserting $p = 2 \, dF/du$ in Eq. (7.20) yields the Arrhenius factor

$$\exp\left(-\frac{2}{\hbar} F(0)\right); \quad (7.22)$$

in accordance with Kramers result in Eq. (7.16).

Finally, eliminating p in the coupled equations (7.18) and (7.19) we obtain the Newton equation of motion

$$\frac{d^2 u}{dt^2} = -\frac{1}{2} \frac{d}{du} \left(\frac{dF}{du} \right)^2; \quad (7.23)$$

for the motion of a particle of mass $1/2$ in the potential $(1/2)(dF/du)^2$. In Fig. 11 c) we have shown the potential which for a double well free energy possesses three maxima at $u = 0$ and $u = \pm 1$. As indicated in Fig. 11 c) the long time orbit from A to B is associated with the long waiting time at the maximum for $u = 0$.

C. Transitions in the Ginzburg-Landau case

In order to induce a non-equilibrium kinetic transition across the free energy landscape in the Ginzburg-Landau case we fix the initial configuration $u_1(x)$ at time $t = 0$ and the final configuration $u_2(x)$ at time T . There are two fundamental issues: 1) the determination of the kinetic pathways and 2) the evaluation of the transition rate. Generally, in order to minimize the free-energy cost, the pathway passes via saddle points, i.e., the multi-domain wall excitations, in the free energy landscape. The actual path chosen, however, depends on the time T allocated to the transition. The transition rate is determined by the Arrhenius factor $\exp(-2F)$ associated with the free energy F of the saddle points encountered along the pathway. In addition there is a prefactor determined by the attempt frequencies; this issue, however, is not dealt with in the present context.

Focussing on a kinetic transition or switch between the two ground states $u = -1$ and $u = +1$ the pathway corresponds to nucleation of domain walls and their subsequent propagation across the system. Let us first consider the case of fixed boundary conditions $u = 0$ at $x = 0$ and $x = L$. The ground state configurations are depicted in Fig. 9 b). In the presence of noise the ground states are metastable and the system can switch from $u = -1$ to $u = +1$ by means of the propagation of a single domain wall across the sample in the transition time T . As discussed above the profiles close to the boundaries over a healing length of order k_0^{-1} correspond to half domain walls and the free energy of either ground state is equal to $F_{dw} = m$, $m = 4k_0/3$; note that for periodic boundary conditions as depicted in Fig. 9 a) the free energy of the ground states vanishes. In order to effectuate a transition a domain wall must nucleate at either boundary and subsequently propagate across the system. The nucleation free energy is $F_{dw} = m$ and from our discussion of the Kramers case we infer the Arrhenius factor $\exp(-2m)$ or within the dynamical description a nucleation action of the order

$$S_{nuc1} = 2m; \quad (7.24)$$

Within the conventional stochastic description the noise generates both the nucleation and the subsequent diffusion of the domain wall across the sample. Since the domain wall carries a finite energy we must within the dynamical description assign a finite energy or finite noise field $p(x)$ at $t = 0$ in order to ensure propagation of the domain wall. Considering the case where the right hand domain wall nucleates at $x = 0$, we assign the noise field $p(x)/p_0 = \cosh^2 k_0 x$ given by Eq. (5.17) at time $t = 0$. In terms of the momentum $p_0 = \hbar m^{1/2}$ given by Eq. (5.19) we thus obtain the velocity $v = p_0/m$, energy $E_0 = p_0^2/2m$, and action by Eq. (6.3), i.e., $S_0 = T \, p_0^2/2m$. The constraint that the system

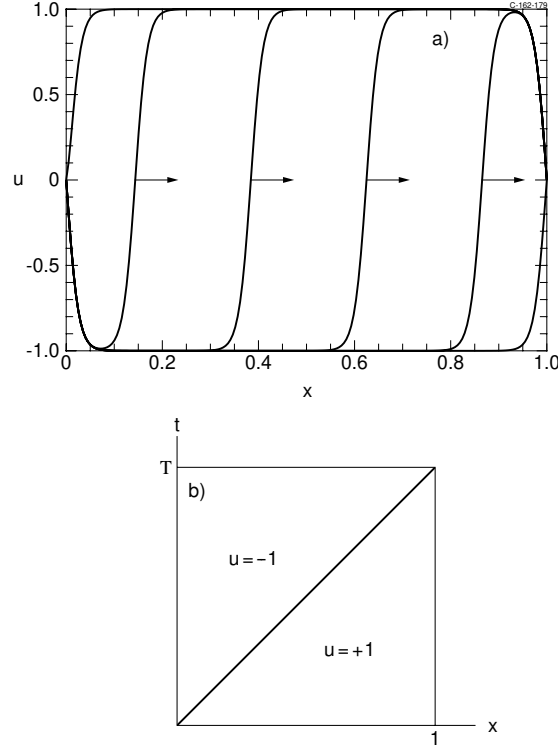


FIG. 12: In a) the switching from $u = +1$ to $u = -1$ in time T is effected by means of a right hand domain wall propagating with velocity $v = 1/T$. The domain wall is nucleated at $x = 0$ and annihilated at $x = 1$. In b) the process is depicted in an $(x;t)$ plot.

of size L is switched at time T moreover impose a selection rule on the propagation velocity. We infer $v = L/T$ and obtain the action $S_0 = m L^2/2T$ associated with the transition. The total action associated with a single domain wall switch is thus given by

$$S_1(T) = S_{\text{nuc1}} + \frac{m L^2}{2T} : \quad (7.25)$$

In Fig. 12 we have in a) depicted the propagation of a single right hand domain wall across the sample. In b) we have shown the transition in an $(x;t)$ plot. In the present case with fixed boundary conditions the momentum p_0 associated with the motion of the domain wall is generated at the boundary $x = 0$ at time $t = 0$ and, subsequently, absorbed at the boundary $x = L$ at time $t = T$. The momentum is given by Eq. (5.13), i.e., $p_0 = p_0 \int dx u_{\text{dw}} \frac{d u_0}{d x}$. Inserting u_0 and u_{dw} given by Eqs. (5.8) and (2.7), respectively, and performing a partial integration using $\int dx \cosh^4 k_0 x = 4/3k_0$ we obtain $p_0 = \frac{4}{3} m^{1/2} > 0$ since $p_0 < 0$ for a positive propagation velocity. Correspondingly, the momentum is absorbed at $x = L$.

For fixed boundary conditions the transition from $u = -1$ to $u = +1$ can also take place by means of nucleation of two domain walls at both ends of the system. The domain walls subsequently propagate towards one another and annihilate at $x = L/2$. The scenario is shown Fig. 13. Since the action is additive for the two-domain wall system the nucleation action is given by $2S_{\text{nuc1}} = 2m$. However, in order to effectuate the transition in time T the velocity is half the velocity in the single domain wall case and we obtain for the action associated with the 2-domain wall transition

$$S_2(T) = 2S_{\text{nuc1}} + \frac{m L^2}{4T} : \quad (7.26)$$

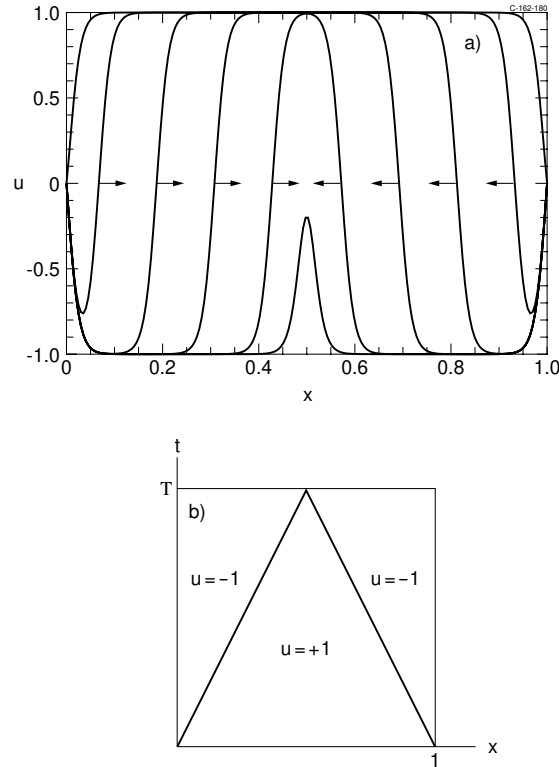


FIG. 13: In a) the switching from $u = +1$ to $u = -1$ in time T takes place by means of two domain walls propagating in opposite directions with velocity $v = 1/2T$. The domain walls nucleate at the boundaries and annihilate at the center. In b) the switching process is depicted in an $(x;t)$ plot.

Finally, in the general case of a transition from $u = +1$ to $u = -1$ in time T by means of the nucleation and propagation of n domain walls the nucleation action is nS_{nuc1} and the domain walls move with velocity $L=T/n$; we obtain the action

$$S_n(T) = nS_{\text{nuc1}} + \frac{mL^2}{2nT} : \quad (7.27)$$

In Fig. 14 we have in an (xt) plot shown a 4-domain wall switch.

In addition to domain wall modes time-dependent localized deformation and extended dispersive modes are also excited, corresponding to small Gaussian fluctuations about the local minima and saddle points and the transition pathway from $u = +1$ to $u = -1$ proceeds by propagating domain walls with superposed linear modes subject to energy and momentum conservation and topological constraints. The energy of the initial state is given by $E = (1/2) \int dx p^2$ and the noise field thus has to be assigned initially in order to reach the switched state $u = -1$ in a prescribed time T . For topological reasons the domain walls must nucleate and annihilate in pairs subject to absorption or radiation of linear modes, respectively. Since the linear modes also carry positive action the dynamical modes with lowest action correspond to nucleation or annihilation of domain wall pairs with equal and opposite momenta, i.e., equal velocities.

In the case of periodic boundary conditions the momentum $\int dx u @ p = @ x$ of the initial and final states is zero. The system is translational invariant and the formation and annihilation of one or several domain wall pairs moving with the same speed take place at equidistant positions along the axis. For fixed boundary conditions the translational invariance is broken and the momentum is nonvanishing corresponding to nucleation and annihilation of domain walls at the boundaries. This general scenario of switching is completely consistent with the numerical analysis in

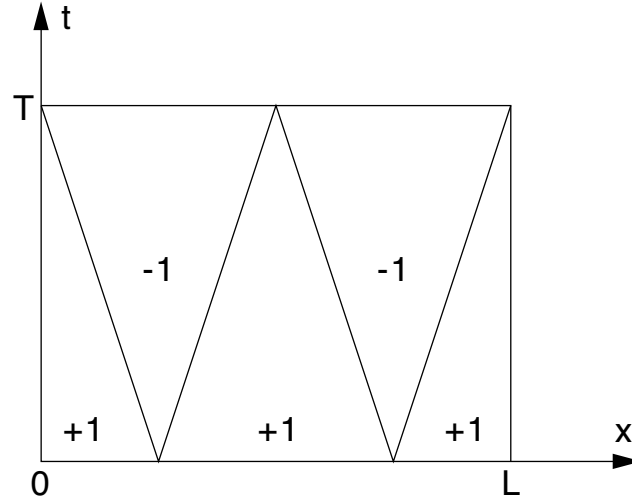


FIG. 14: We show a 4-domain wall switch in an $(x; t)$ plot.

[21].

1. Improved estimate of S_{nuc1}

The above estimate of the nucleation action S_{nuc1} for a domain wall was based on an analogy with the Arrhenius factor in the simple Kramers case of escape from a potential well. Here we improve the estimate of S_{nuc1} based on the phase space formulation. We consider the case of a switch from $u = +1$ to $u = -1$ in time T proceeding by 1) the nucleation of two domain walls at the center of the system during the time interval τ , 2) propagation of the domain walls with opposite velocities during the time interval $T - \tau$, and 3) the annihilation of the domain walls at the boundaries during the time interval τ . From the width of a single domain wall k_0^{-1} and the propagation velocity $v = L/2T$ we estimate the nucleation time, i.e., the time it takes for the nucleation to separate in two distinct domain walls, to be of order $\tau = 2/vk_0 = 4T = k_0 L$. From Eq. (3.10) the nucleation action per domain wall is given by

$$S_{\text{nuc1}} = \frac{1}{2} \int_{u=+1,0}^{u=-1,T} dx dt (p du = dt - H); \quad (7.28)$$

where u is the nucleation configuration just prior to breaking up into two domain walls; H is the energy density which we determine below. In order to estimate S_{nuc1} we consider the field equations (4.1) and (4.2). The initial configuration is $u(x) = u(x; t=0) = 1$ and denoting the initial noise field by $p_0(x) = p(x; t=0)$ and, moreover, considering a large system so that τ is small, we obtain to leading order in τ from the equations of motion

$$u(x; t) = \frac{\partial^2 u(x; t)}{\partial x^2} + 2k_0^2 u(x; t) (1 - u(x; t)^2) + p_0(x) \quad t + 1; \quad (7.29)$$

$$p(x; t) = \frac{\partial^2 p(x; t)}{\partial x^2} - 2k_0^2 p(x; t) (1 - 3u(x; t)^2) \quad t + p_0(x); \quad (7.30)$$

or by insertion

$$u(x; t) = p_0(x) \quad t + 1; \quad (7.31)$$

$$p(x; t) = \frac{\partial^2 p}{\partial x^2} + 4k_0^2 p_0(x) \quad t + p_0(x); \quad (7.32)$$

These solutions describe the initial part of the orbit in (up) phase space corresponding to the nucleation of two domain walls. The unspecified initial noise field $p_0(x)$ acts as an initiator. The noise profile $p_0(x)$ is localized at the position of the nucleation. Since the orbit lies on an energy surface we have $E_0 = (1/2) \int dx p_0(x)^2$ and we infer the energy

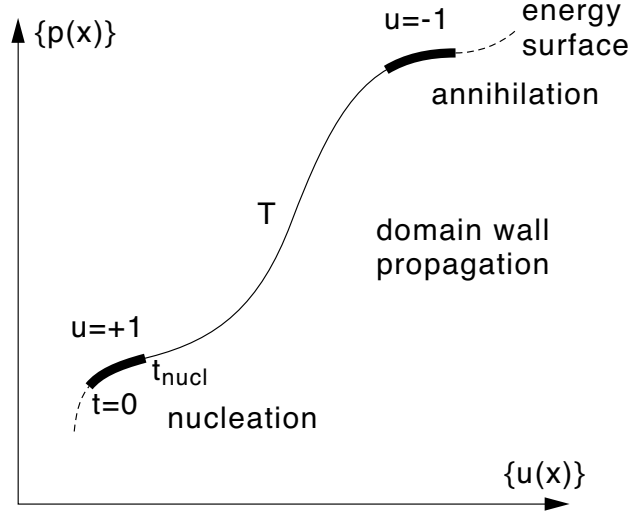


FIG. 15: We sketch the orbit in phase space corresponding to the nucleation of a domain wall pair during time t_{nuc} , the subsequent propagation across the system during time $T \gg t_{\text{nuc}}$, and the final annihilation of the individual domain wall at the boundaries during time t_{nuc} .

density $H = (1/2)p_0(x)^2$. From the equation of motion $du(x)/dt = p_0(x)$ and inserting in the action in Eq. (7.28) we obtain $S_{\text{nuc}} = (1/2) \int dx [p_0(x) + (\partial_x^2 p_0(x) = \partial_x^2 + 4k_0^2 p_0(x)) t] p_0(x) - (1/2) \int dx p_0(x)^2$. Rearranging and performing a partial integration, assuming $p_0(x)$ localized, we find the following expression for the nucleation action per domain wall:

$$S_{\text{nuc}} = \frac{1}{2} t E_0 + \frac{1}{2} (t^2 - 8k_0^2 E_0 + \int dx \frac{(\partial_x p_0(x))^2}{\partial_x} : \quad (7.33)$$

This is a short time estimate and holds for a large system, i.e., for $k_0 L \gg 1$. The energy $E_0 = 2(1/2)m v^2$ is found from the 2-domain wall sector. Inserting $t = 4T = k_0 L$, $v = L/2T$, $m = 4k_0 = 3$, estimating $(\partial_x p_0(x) = \partial_x)^2 = f k_0^2 p_0(x)^2$, where f is a "fudge" factor of order one, and lumping the term linear in t with the domain wall pair propagation, we obtain $S_{\text{nuc}} = t^2 (4 + f) k_0^2 E_0$. Further reduction yields the result

$$S_{\text{nuc}} = (4 + f) m \quad (7.34)$$

This expression for the nucleation action has the same form as the one derived from the simple Kramers theory. In Fig. 15 we have in a phase space plot sketched the orbit and indicated the nucleation, propagation, and annihilation regions.

VIII. INTERPRETATION OF NUMERICAL RESULT

Here we make contact with the numerical analysis of the Ginzburg-Landau equation by E, Ren, and Vandeneijnden [21]. These authors analyze the noise induced switching by means of an optimization techniques applied to the Freidlin-Wentzel action

$$S_{\text{FW}} = \frac{1}{2} \int_0^L dx \int_0^T dt \left[\frac{(\partial_t u)^2}{\partial_t} + \frac{(\partial_x^2 u)^2}{\partial_x^2} + 2k_0^2 u(1 - u^2) \right] : \quad (8.1)$$

for a system of size $L = 1$ over a time span T and find that the global minimum of S_{FW} corresponds to the nucleation and propagation of domain walls. First we observe that the minimizing configurations, the minimizers, of (8.1) are identical to the orbits found within the canonical phase space approach. This correspondence was discussed in Sec. III and is seen by noting that insertion of the equation of motion for p and the Hamiltonian (4.3) in the expression for the action (3.10) yields the Freidlin-Wentzel form in (8.1).

Switching a system of size L in time T by means of a single domain wall, corresponding to the pathway via the lowest local minimum of the free energy at $F_{dw} = m$, the propagation velocity $v = p_0/m = L/T$ and we obtain the action $S_1(T) = S_{nuc1} + mL^2/2T$ in Eq. (7.25) and associated transition probability

$$P \sim \exp \left(-\frac{S_{nuc1}}{k_0} - \exp \left(-\frac{mL^2}{2T} \right) \right) : \quad (8.2)$$

In the thermodynamic limit $L \rightarrow \infty$, $P \rightarrow 0$ as a result of the broken symmetry in the double well potential. At long times the action falls off as $1/T$. At intermediate times t and positions x we have $P \sim \exp(-mx^2/2t)$ and the domain wall in the stochastic interpretation performs a random walk with mean square displacement $2t/m$, corresponding to diffusive behavior. In Fig. 12 a we have shown a domain wall nucleating at the left boundary and propagating with constant velocity $v = L/T$ to the right boundary, where it annihilates. We have used the same parameter values as in [21], i.e., $m = 0.3$, $2k_0^2 = 1$, $T = 7$, and a system size $L = 1$. In Fig. 12 b we have plotted the trajectory of the domain wall in space and time.

The switching can also take place by nucleating two domain walls at the boundaries. These then move at half the velocity $v=2$ and subsequently annihilate at the center. This process corresponds to the pathway via the local saddle point of the free energy at $F_{dw} = 2m$, and the action is given by $S_2(T) = 2S_{nuc1} + 2S_1(4T)$ in Eq. (7.26). The associated transition probability is

$$P \sim \exp \left(-\frac{2S_{nuc1}}{k_0} - \exp \left(-\frac{mL^2}{4T} \right) \right) : \quad (8.3)$$

Snapshots of this process are shown in Fig. 13 a and the corresponding space-time plot in Fig. 13 b.

Combining the contributions from nucleation and the subsequent domain wall propagation we obtain the heuristic expression in Eq. (7.27), where S_{nuc} is the action for nucleating a single domain wall and n is the number of walls. From the improved estimate of S_{nuc1} in Eq. (7.34) with fudge factor $f = 1$ we have

$$S_{nuc} \approx 5k_0 : \quad (8.4)$$

In Fig. 16 we have plotted S versus T for $n = 1 \dots 6$ domain walls using the parameter values in [21]. Choosing S_{nuc} according to (8.4) we find excellent agreement with the numerical results.

As also discussed in [21] we note that the switching scenario depends on T . At shorter switching times it becomes more favorable to nucleate more domain walls. In the present formulation this feature is associated with the finite nucleation or annihilation action S_{nuc} . This is evidently a finite size effect in the sense that the action at a fixed T diverges in the thermodynamic limit $L \rightarrow \infty$, corresponding to the broken symmetry.

IX. SUMMARY AND CONCLUSION

In the present paper we have implemented the dynamical phase space approach developed previously for the noisy Burgers equation to the case of the one dimensional noise-driven Ginzburg-Landau equation. Based on a linear analysis of the static domain wall solutions in the noiseless case we find that the kinetic transitions take place by means of propagating multi-domain wall configurations with superimposed local deformation and extended diffusive modes. The approach also allows for a determination of the Arrhenius factor associated with the transitions. The motivation for the present work is a recent numerical optimization study by E. et. al. [21] of the noisy one dimensional Ginzburg-Landau equation based on the Freidlin-Wentzel theory of large deviations. We find excellent agreement both qualitatively and quantitatively with the numerical finding of E. et al. [21]. The dynamical approach offers in the nonperturbative weak noise or low temperature limit an alternative way of determining dynamical pathways and the Arrhenius part of the associated transition rates.

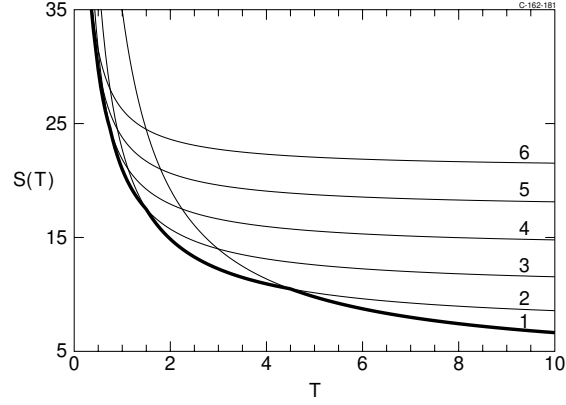


FIG. 16: The action $S(T)$ given by (7.27) is plotted as a function of T for transition pathways involving up to $n = 6$ domain walls. The lowest action and thus the most probable transition is associated with an increasing number of domain walls at shorter times, indicated by the heavily limiting curve. The curves correspond to choosing $S_{\text{nuc}} = 5 k_0$.

-
- [1] P. L. Geissler, C. Dellago, D. Chandler, J. Hutter, and M. Parrinello, *Science* 291, 2121 (2001).
 - [2] D. V. Berkov, *J. Magn. Magn. Mat.* 186, 199 (1998).
 - [3] R. H. Koch, G. Grinstein, G. A. Keefe, Y. Lu, P. L. Trouilloud, W. J. Gallagher, and S. S. P. Parkin, *Phys. Rev. Lett.* 84, 5419 (2000).
 - [4] C. Jaffe, S. Ross, M. W. Lo, J. Marsden, D. Farrell, and T. Uzer, *Phys. Rev. Lett.* 89, 011101 (2002).
 - [5] P. Hanggi, P. Talkner, and M. Borkovec, *Rev. Mod. Phys.* 62, 251 (1990).
 - [6] M. I. Freidlin and A. D. Wentzel, *Random Perturbations of Dynamical Systems* (2nd ed. Springer, New York, 1998).
 - [7] S. Machlup and L. Onsager, *Phys. Rev.* 91, 1512 (1953).
 - [8] L. Onsager and S. Machlup, *Phys. Rev.* 91, 1505 (1953).
 - [9] R. Graham and T. Tel, *J. Stat. Phys.* 35, 729 (1984).
 - [10] R. Graham and T. Tel, *Phys. Rev. A* 42, 4661 (1990).
 - [11] P. C. Martin, E. D. Siggia, and H. A. Rose, *Phys. Rev. A* 8, 423 (1973).
 - [12] C. de Dominicis, *Phys. Rev. E* 12, 567 (1975).
 - [13] C. de Dominicis, *J. Phys. (Paris), Colloq.* 37, 247 (1976).
 - [14] R. Baussch, H. K. Janssen, and H. Wagner, *Z. Phys. B* 24, 113 (1976).
 - [15] H. K. Janssen, *Z. Phys. B* 23, 377 (1976).
 - [16] C. de Dominicis and L. Peliti, *Phys. Rev. B* 18, 353 (1978).
 - [17] P. G. Bolhuis, D. Chandler, C. Dellago, and P. Geissler, *Ann. Rev. of Phys. Chem.* 59, 291 (2002).
 - [18] W. Ren (2002), PhD Thesis (unpublished).
 - [19] W. E, W. Ren, and E. Vanden-Eijnden, *Phys. Rev. B* 66, 052301 (2002).

- [20] J. Garcia-Ojalvo and J.M. Sancho, *Noise in Spatially Extended Systems* (Springer, New York, 1999).
- [21] W. E, W. Ren, and E. Vanden-Eijnden (2002), *cond-mat/0205168*.
- [22] H.C. Fogedby, A.B. Eriksson, and L.V. Mikkelsen, *Phys. Rev. Lett.* 75, 1883 (1995).
- [23] H.C. Fogedby, *Phys. Rev. E* 57, 4943 (1998).
- [24] H.C. Fogedby, *Phys. Rev. Lett.* 80, 1126 (1998).
- [25] H.C. Fogedby, *Europhys. Lett* 56, 492 (2001).
- [26] H.C. Fogedby, *Eur. Phys. J. B* 20, 153 (2001).
- [27] H.C. Fogedby, *Phys. Rev. E* 68, 026132 (2003).
- [28] H.C. Fogedby and A. Brandenburg, *Phys. Rev. E* 66, 016604 (2002).
- [29] H.C. Fogedby, J. Hertz, and A. Svane, *Europhys. Lett* 62, 795 (2003).
- [30] A.J. Bray, *Adv. Phys.* 43, 357 (1994).
- [31] M.C. Cross and P.C. Hohenberg, *Rev. Mod. Phys* 65, 851 (1994).
- [32] R.S. Maier and D.L. Stein, *Phys. Rev. Lett.* 87, 270601 (2001).
- [33] S. Habib and G. Lythe, *Phys. Rev. Lett.* 84, 1070 (2000).
- [34] H.C. Fogedby, P. Hedegaard, and A. Svane, *Physica B* 132, 17 (1985).
- [35] H.C. Fogedby, *Phys. Rev. E* 59, 5065 (1999).
- [36] R. Rajaraman, *Solitons and Instantons* (North-Holland, Amsterdam, 1987).
- [37] H.A. Kramers, *Physica* 7, 284 (1940).